

Design of a 175 GHZ SiGe-based voltage-controlled oscillator with greater than 7.6 dBm power

Oluseun Damilola Oyeleke^{1,2}, Aliyu Danjuma Usman², Kabir Ahmad Abubilal², Habeeb Bello²,
Olabode Idowu-Bismark³

¹Department of Computer Engineering, Nile University of Nigeria, Abuja, Nigeria

²Department of Electronic and Telecommunication Engineering, Ahmadu Bello University, Zaria, Nigeria

³Department of Electrical and Information Engineering, Covenant University, Ota, Nigeria

Article Info

Article history:

Received Nov 8, 2022

Revised Nov 28, 2022

Accepted Dec 30, 2022

Keywords:

Colpitts oscillator

Microwave

SiGe 130 nm

Terahertz

Voltage controlled oscillator

ABSTRACT

In this research, we present a low phase noise (PN) and wide tuning range 175 GHz inductors and capacitors (LC) voltage-controlled oscillator (VCO) based on a differential Colpitts oscillator that was designed using a 0.13 μm bipolar complementary metal oxide semiconductor (BiCMOS) and simulated. The square of the tank Q-factor and the square of the oscillation amplitude were both maximized to reduce PN. With an extensive examination of parasitic, mathematical analysis of load impedances, and implementation of differential design, the PN was reduced, and the output power was enhanced. Using a supply voltage of 1.6 V, the VCO consumes 41.9 mA, resulting in a total power usage of 67 mW to prevent undesirable PN deterioration, an inter-stage LC filter at the VCO-buffer interface increases the swing at the buffer input. To make a better output, a buffer is used to isolate the load from the VCO core. In addition, the VCO has a high linearity and the overall, the VCO presented in this study demonstrates excellent performance and has the potential to be used in a wide range of applications that require a high-performance, low-power VCO.

This is an open access article under the [CC BY-SA](https://creativecommons.org/licenses/by-sa/4.0/) license.



Corresponding Author:

Olabode Idowu-Bismark

Department of Electrical and Information Engineering, Covenant University

Ota, Ogun State, Nigeria

Email: idowubismarkolabode@gmail.com

1. INTRODUCTION

The terahertz (THz) spectrum is the next frontier for efficient imaging applications [1], [2] and high-bandwidth wireless communication [3]. THz radiation has a greater spatial resolution for imaging and sensing than lower-frequency radio and millimeter waves due to its shorter wavelength [4], [5]. Another notable aspect is that the permittivity of various materials can be determined by measuring their spectral response to THz radiation. As more applications are being explored and deployed at THz frequencies, there will be a demand for devices able to generate and amplify signals at THz frequencies. One of the major obstacles to achieving any of the uses is the creation of high-power, integrated THz sources that operate inside the THz atmospheric transmission windows [6]. For the realization of these THz cameras, high powered signal sources are necessary.

The seventh framework programme (FP7) for research and technology, 700 GHz has been identified by European commission development as a promising solution for mmWave imaging and sensing [7]. Terasense, a leading company in THz imaging identified the 700 GHz region as a part of the electromagnetic (EM) frequency spectrum where most common materials are transparent to THz radiation. A previous researcher's goal was to use common-mode impedance enhancement to construct a 300 GHz Silicon-

Germanium (SiGe-based) high-performance push-pull voltage controlled oscillator (VCO) with >1 -mW peak power output, which is a novel way of enhancing the efficiency and power output THz signal sources and millimeter-wave and. To greatly increase the harmonic power output compared to a conventional method, this research will demonstrate two push-push VCOs based on a unique method for achieving a common-mode resonance in a Colpitts push-push oscillator circuit. The VCOs discussed Wallace *et al.* [8] operate between 292 and 0.318 THz and 0.305 and 0.327 THz, respectively, with peak power outputs of 1.15 and 1.05 mW and an 8% tuning range. This outputs power and tuning range needs improvement to overcome penetration attenuation in body area networks. To be utilized for high-resolution imaging.

Research by Vafapour *et al.* [9] aim to come up with a strategy for creating small, millimeter-wave fundamental oscillators with high efficiency that operate above the active device's $f_{max}/2$ to optimize oscillator output strength. An iterative strategy based on load and source-pull techniques was employed to optimize the amplifier's power output. However, the 65 nm complementary metal oxide semiconductor (CMOS) process was appropriate for applications with low power (LP) options because its gate has a nominal operating voltage of 1.2 V which is a LP option when in comparison with other different foundries 90 nm LP, 90 nm general purpose (GP), and 130 nm GP processes. 65 nm CMOS performance was also degraded by temperature variations.

Research by Chiang *et al.* [10] using analog integrated circuits, this study discusses the construction of a quadrature VCO (QVCO) that can create offset frequencies of positive and negative alterations, as well as zero frequency. It had two integrator loop oscillators and was one of the simplest quadrature-phase oscillator types. Each integrator adjusts the phase by 90 degrees, while negative feedback shifts it by 180 degrees, for a complete 360 degrees phase shift around the loop. However, a major drawback of using a transconductance capacitor was its difficulty in the implementation of a rail-to-rail input capability. (A rail-to-rail output was an output where the value of the output can be the entire range of the power supply) the power consumption can be improved by using SiGe semiconductor processes. Also, the tuning scheme of this transconductance capacitor to achieve good precision was challenging and hence also increases their complexities in implementation.

According to Momeni and Afshari [11] the series-coupled QVCO (SQVCO) was proposed as a modification to the SQVCO to decrease phase noise (PN) in the VCO. To ensure that the switching transistor also affects the tank's rising edge current pulse, hence small capacitors must be added to each cell. However, even employing coupled oscillators, the maximum tuning range was still relatively limited, necessitating the usage of many VCO cores to provide sufficient power output. Research by Voinigescu [12] developed a different fundamental frequency VCO with a 176 GHz central frequency. High power output, low PN, strong linearity, and compacted sizes are among the benefits of the chosen architecture, which is paired with the usage of a Colpitts topology based on common emitters. The tuning bandwidth was 8.5, PN was 110 at 10, maximum power output was 7.3 dBm, maximum output variation was 1.7 dBm, DC power was 82 mW, maximum efficiency was 6.6, and chip measurements were 0.30×0.35 . The tuning range, PN maximum performance, and power output can all be enhanced to roughly 100 mW.

Considering the limitations of the reviews made, the aim of this paper, therefore, is to design, model and simulate a VCO with a $PN < -100$ at 10 MHz dB/Hz, >7 dBm power output, $>3\%$ tuning range at 175 GHz based on the fully-differential, push-push, Colpitts topology. Additional works will extract the 4th harmonic signal from 175 GHz to build a 700 GHz signal generator for imaging. The contribution of this work is to achieve a power output of greater than 7.6 dBm, PN of -73 at 10 MHz offset, a tuning range of 11.9% and a power consumption of 67.18 mW results were achieved.

2. PROPOSED METHOD

A promising scheme to obtain radio frequency (RF) power at 700 GHz is to utilize a low PN G-band-wave oscillator with a high-performance amplifier/multiplier chain. Figure 1 shows the block diagram conceptual model of the proposed integrated 700 GHz THz generator. The choice of the target frequency is based on the frequency at which objects are transparent to THz signals.

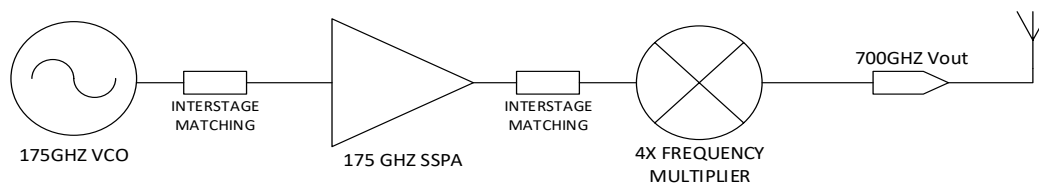


Figure 1. Conceptual design of a 700 GHz signal source

This paper's focus is the development of block one (VCO) of this approach. In realization of the VCO, a differential Colpitts oscillator with power-combined output will be designed and simulated. The figure of merit critical to the efficiency of the VCO is the output power, PN, and tuning range, and hence design will be optimized to maximize these parameters. The steps followed to realize this is parameter extraction of the transistor model, determination of effective impedance, resonant frequency parameters, and reduction of PN.

3. METHOD

3.1. Parameter extraction analysis

It will be impossible to build a VCO at such a high frequency without substantive parameter analysis. One of the main effects of parasitics at high frequency is an increase in the oscillation frequency which causes fluctuations, an increase in the phase noise of the VCO and parasitics can also increase the power consumption of the VCO at high frequencies. This is because parasitics can cause additional current to flow through the circuit, increasing the power consumption of the VCO. Overall, it is important to carefully consider the impact of parasitics in high frequency VCO design. The parametric extraction utilized in this research is shown in Table 1.

Table 1. The small-signal equivalent-circuit parameters [13], [14]

Symbol	Description	Value	Unit
r_π	Small-signal base-emitter resistance	12	Ω
r_B	Base spreading resistance	3	Ω
$C_\pi(C_{be})$	Base-emitter capacitance	7	fF
$C_u(C_{bc})$	Base-collector capacitance	15	fF
C_{var}	Varactor capacitance	50	fF
C_{common}	Common-mode resonant capacitance	16	fF
L_B	Base tank inductance	20	pH
g_m	Small signal transconductance	420	mS
f_T	Transit frequency	300	GHz
I_{bias}	Bias current	40	mA

3.2. Determination of the effective input impedance

In the determination of the effective input impedance of the Colpitts oscillator with parasitics and effective negative resistance for sustained oscillation to determine the overall input impedance of the VCO. The impedances of all active and passive elements are presented. A small equivalent circuit of the heterojunction bipolar transistor (HBT) and a high-frequency equivalent model of the VCO half-circuit shown in schematic simplified for analysis is shown in Figure 2. For ease of derivation of the input impedance Z_{in} , alphabets were assigned to parameters as presented in Table 2 to ensure the equation derived is accurate.

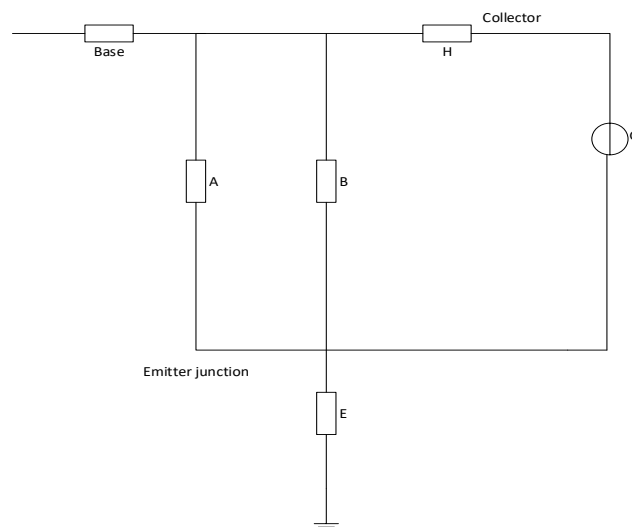


Figure 2. Equivalent model of a high-frequency VCO half-circuit

Table 2. Parameters for the derivation of total input impedance seen at the VCO

Parameters	Alphabet assignment
ZC_{be}	A
r_π	B
$A B$	C
ZC_{qvar}	E
$C + (G + 1)E$	D
ZC_{bc}	H
Z_{Total}	K
K	$D H$
ZC_{be}	$-j \frac{1}{\omega C_{be}}$
ZC_{bc}	$-j \frac{1}{\omega C_{bc}}$
G	$-j \frac{\omega_T}{\omega}$
ZL_B	Base tank inductance ($j\omega L_B$)
r_B	Base spreading inductance

$$C = \frac{AB}{A+B} \quad (1)$$

$$D = \frac{AB}{A+B} + (G + 1)E \quad (2)$$

$$D = \frac{AB}{A+B} + (G + 1)E \quad (3)$$

$$K = \frac{H(AB+E(GA+GB+A+B))}{A(B+GE+E+H)+B(GE+E+H)} \quad (4)$$

$$Z_{total} = \frac{ZC_{bc}(ZC_{be}r_\pi + ZC_{be}\frac{\omega_T}{\omega} + ZC_{bc}\frac{\omega_T}{\omega} + ZC_{qvar})}{ZC_{be}(r_\pi + ZC_{bc}\frac{\omega_T}{\omega} + ZC_{bc}\frac{\omega_T}{\omega} + ZC_{qvar})} \quad (5)$$

$$Z_{in} = Z_{total} + j\omega L_B + r_B \quad (6)$$

where, $Z_{total} = R_{total} + jX_{total}$ note that R_{total} this is the real part Z_{total} which also includes r_b . A method used to generate a negative resistance was by adding reactive elements from transmission lines at the base of the transistor and hence total negative resistance which will develop at the base of the active device is:

$$R_{-ve} = R_{total} + r_b \quad (7)$$

When the negative resistance is present, the requirement for oscillation is satisfied. At the oscillation frequency, R_{total} adjusts for resonator losses.

3.3. Determination of the resonant frequency parameters

To determine the resonant frequency based on the design of the Colpitts oscillator, a reduced tank circuit schematic is shown for analysis as shown in Figure 3.

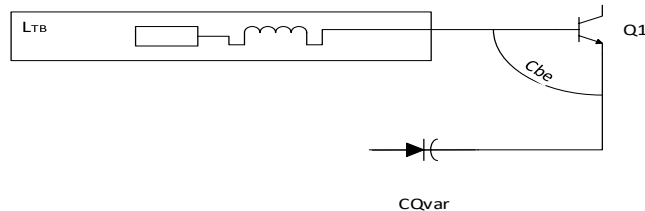


Figure 3. Colpitts tank circuit with parasitic capacitances

For oscillation to occur all reactance must equal zero [15]:

$$X_{Cbe} + XL_{TB}C_{Qvar} = 0 \quad (8)$$

After some algebraic analysis, as (8) reduces to:

$$\frac{1}{\omega} = \sqrt{(L_{TB}) \left[\frac{C_{be}C_{qvar}}{C_{be}+C_{qvar}} \right]} \quad (9)$$

There is contact parasitic L_{par} in series with L_{TB} and ignoring mutual inductance as (9) is recast as:

$$\frac{1}{\omega} = \sqrt{(L_{TB} + L_{par}) \left[\frac{C_{be}C_{qvar}}{C_{be}+C_{qvar}} \right]} \quad (10)$$

Where, C_{be} and C_{bc} are parasitic capacitances, C_{qvar} is varactor capacitance, with the condition in (10) met and the values of L and C set the circuit will start oscillating at the center frequency of 175 GHz.

3.4. Estimation of the simplified fundamental oscillation condition negative resistance

The negative resistance generated by the transistors compensates for the resistive losses in the passive parts, allowing the oscillation to continue (Q1 and Q2). In a VCO, an oscillator occurs when all reactive components cancels and only real resistance between the LC tank circuit and resistance of the active device are left in the system [16], [17]. To ensure that oscillation will occur and is sustained, the negative resistance developed at the base of the transistor was carefully set. The small signal negative resistance at the transistor's base can be expressed as [18], [19]:

$$R = \Re(Z_{in}) = \frac{-g_m}{\omega^2 C_1 C_2} \quad (11)$$

For a practical HBT, the total resistance required to supply negative resistance is made up of a summation of R_{par} , R_s , and r_b , and hence as (11) can also be given in the form as (12) [20]:

$$R = \frac{g_m}{\omega_{osc}^2 C_{BE} C_{var} R_{par} R_s} \quad (12)$$

Where, R_{par} and L_{par} are the parasitic impedances of the connections between the thick metal layers typically employed for microstrips and the transistor contact layers, respectively. r_b and R_s are the series resistance of transmission lines and transistor base spreading resistance. L_{TL} is the inductance of the transmission line. This implies that the net resistance between the tank and the active device is almost equal to 0 so that the active device produces resistance to compensate for the loss of resistance by the tank circuit. if this is not done the oscillation is not sustainable.

3.5. Reduction of phase noise

In this section, the PN is reduced. The VCO PN is a function of the oscillation amplitude, C_1 , the C_1/C_2 ratio, and of I_n . The total equivalent input noise current of the transistor as given by [21].

$$\frac{P_{noise}}{P_{AVS}} = \frac{|I_n^2|}{V_{osc}^2 f_m C_1^2 (C_1+1)^2} \quad (13)$$

When C_1 is dominated by C_{be} , the bipolar junction transistor (BJT) transformation as (13) was given by [22].

$$\frac{P_{noise}}{P_o} = \frac{|I_n^2|}{V_{osc}^2 f_m^2 C_{BE}^2 \left(\frac{C_{be}}{C_{qvar}} \right)^2} \quad (14)$$

where, V_{OSC} is the tank voltage amplitude, P_{noise} output noise power, f_m is the frequency offset, P_{AVS} is the power of the carrier.

PN is in inverse proportionality to the square of the tank Q and the square of the oscillation amplitude V_{OSC} , both were maximized. According to as (14), increasing the size of the HBT causes the oscillation frequency to decrease. The VCO PN performance is determined by the values of C_π (which is dominated by C_{be}) and Q_{var} , as well as the oscillation amplitude and equivalent input noise current of the HBT (I_n).

3.6. Selection of the voltage-controlled oscillator topology

The differential Colpitts topology was applied, as illustrated in Figure 4. The differential design is more suited to integrated circuit implementations. Particularly where power supply noise and substrate noise coupling are to be minimized.

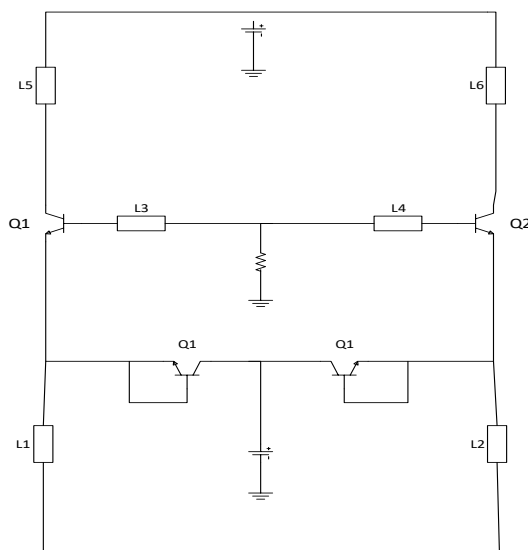


Figure 4. Fully differential voltage control Colpitts oscillator architecture

A differential topology has benefits in terms of quality factor and tuning range, and by power combining, additional 3 dB power can be obtained. The designed VCO core shown in Figure 5 comprises transistors Q1, and Q2 and the resonator, which is composed of an inductor $L_{3,4}$. Which includes the parasitics contacts and an effective capacitance. An oscillator with a tank circuit is formed by a connection of matched transistors in a differential arrangement. The tuning voltage at the base of Qv₁ and Qv₂ is used to alter their capacitances and provide a wide tuning range. The SG132 HBT active device was utilized to provide a quantity of energy that was equal to the energy dissipated, allowing the circuit to maintain oscillations.

3.7. Design of output buffer design

The buffer was realized with a simple common collector scheme as shown in Figure 5. The buffer helps provide separation between the external load and VCO core and VCO pulling, like pushing, was kept to a minimum topology with built-in isolation between the VCO tank and the load hereby providing a strong reverse-isolation. The buffer is completely symmetrical. The VCO core and the buffer are both powered at the same voltage. Because the voltage supply was kept as low as possible, an output buffer stage and separate VCO core were used instead of the typical stacked buffer technique (1.6 V). At these frequencies, VCOs are commonly constructed without output buffers, which provides excellent performance without significantly affecting power consumption and allows for the use of a lower bias voltage, enhancing the monolithic microwave integrated circuit (MMIC) system integration.

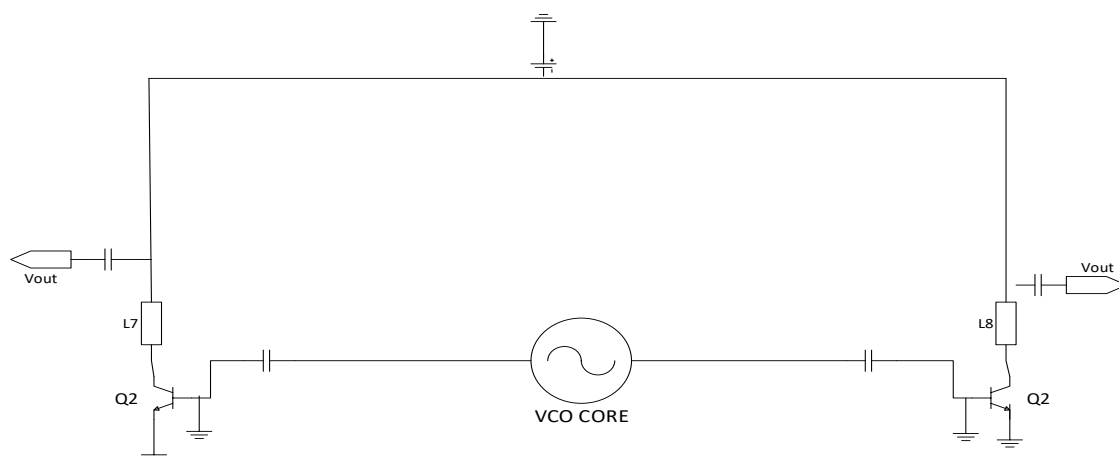


Figure 5. VCO buffer design

3.8. Designing of varactors for voltage-controlled oscillator tuning range

To achieve wider frequency operations and take advantage of the available bandwidth, the oscillator was designed to cover the center frequencies of each channel with some margin. The usage of varactors to cover the bandwidth provides an easy answer to this tuning range requirement. A big varactor would diminish the tank's quality factor and therefore the PN because the varactor loss is considerable at mm-waves due to huge ohmic losses. The variable capacitance in this design was obtained by connecting two transistors Q_1 (Q_{var5} and Q_{var6}) with short-circuited base-emitter junctions to create back-to-back diode configuration as shown in Figure 6 in an anti-series configuration, which improves the Colpitts VCO's tunability and linearity. With dimensions of $0.07 \times 6.3 \times 7 \mu\text{m}^2$ each. The varactor takes an input voltage of 800 mV and 16 pA which makes the VCO tunable with low voltage and power consumption. Furthermore, each of these transistors is constructed at the layout level using a pair of parallel transistors using the same dimensions as Q_1 and Q_2 to reduce losses caused by the resonator tank.

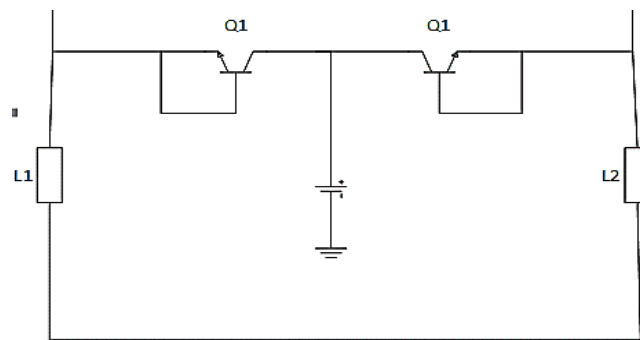


Figure 6. 175 GHz varactor design

3.9. Designing of the final circuit diagram of voltage-controlled oscillator

A differential structure has advantages in terms of quality factor and tuning range, and power combining can provide an additional 3 dB of power. Because it was designed with a differential architecture, the circuit layout is precisely symmetrical as shown in Figure 7, and because the active device is biased to have negative resistance, the overall resistance of the resulting parallel resonant circuit is negative. Q_1 and Q_2 are sized and biased individually for the best noise and oscillation amplitude. The final layout of the VCO is shown in Figure 8.

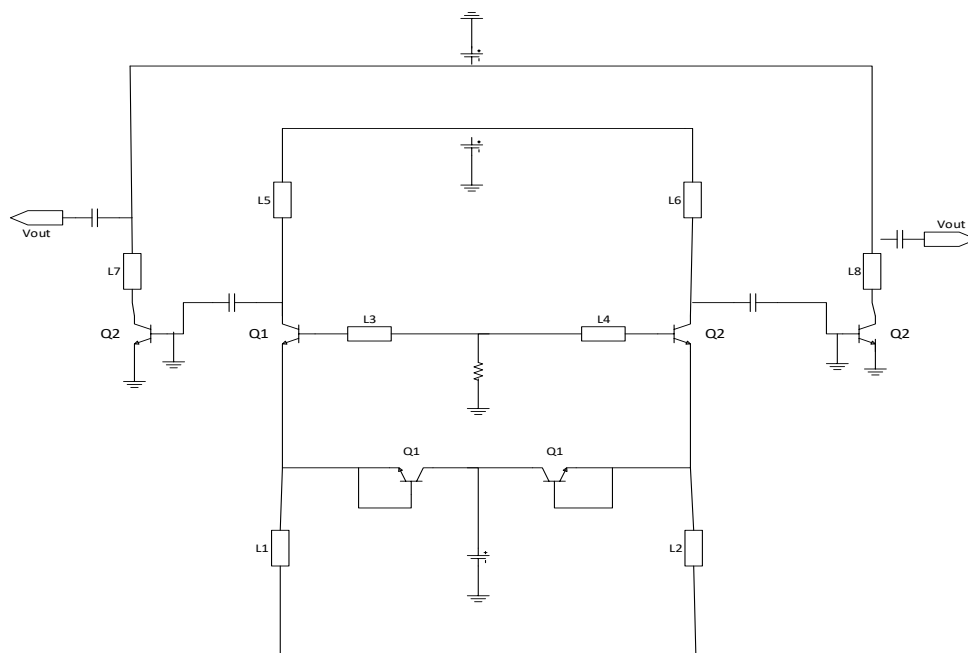


Figure 7. Complete 175 GHz differential VCO design

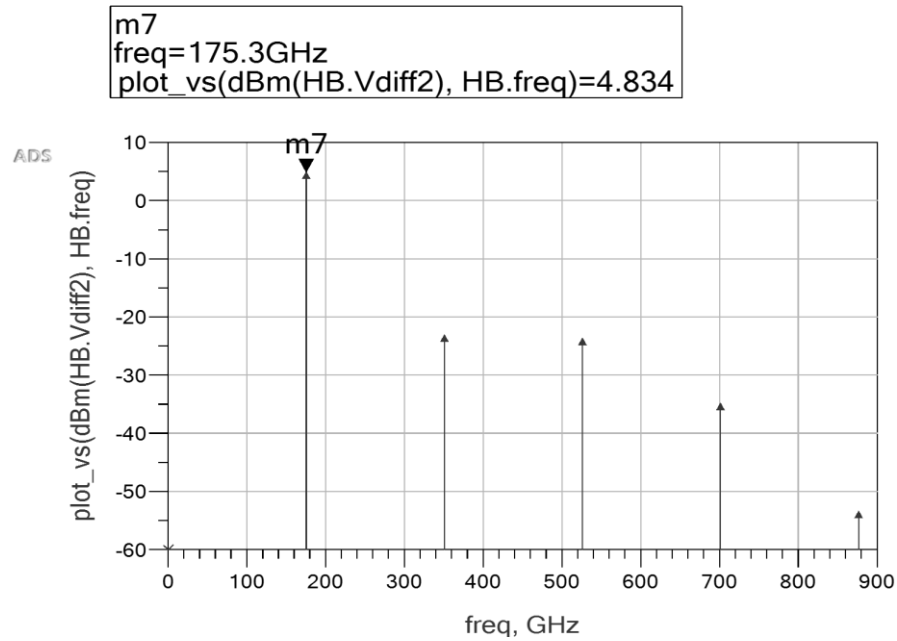


Figure 8. Differential power output1 (175.3 GHz and 4.834 dBm (3.04 mw))

3.10. Simulation setup

Advanced design system (ADS) keysight 2019. The IHP SG132 product development kit was used for the simulation of the VCO. The parameters used for the design are presented in Table 3.

Table 3. Chosen parameter values for 175 GHz VCO design and simulation

Parameter	Value	Unit
$Q_1, Q_2 (w \times l)$	$0.07 \times 0.09 \times 8$	μm^2
$QVar_{5-6} (w \times l)$	$0.07 \times 0.09 \times 9$	μm^2
R	>100	Ω
L_B	20	pH
gm	33	mS
I_{bias}	42.6	mA
V_{osc}	919	mV
V_{cc}	1.6	V
$L_{1,2} (l \times w)$	100×2	μm^2
$L_{3,4} (l \times w)$	59.5×2	μm^2
$L_{5,6} (l \times w)$	15×4	μm^2
$L_{7,8} (l \times w)$	62×4	μm^2

4. RESULTS AND DISCUSSION

4.1. Results of power output

The circuit's frequency response in Figure 8 reveals a peak power output of close to 5 dBm at 175 GHz. The differential output voltages are symmetrical which is very important to have balanced operation and added power. An output-to-input power ratio of 2:1 translates into a gain of 3 dB when the signal strength is doubled. The peak of 7.834 dBm output power is high, given the fact that the overall DC-power consumption of the VCO is 67 mW only.

4.2. Results of phase noise

The VCO's PN performance which is a very important metric in the performance of a VCO was also simulated; the simulated results are shown in Figure 9. In this case, the fundamental signal is at 175 GHz, and the bias voltage is 1.6 V. A PN of -73.90 dBc/Hz was simulated with this arrangement at a frequency offset of 10 MHz.

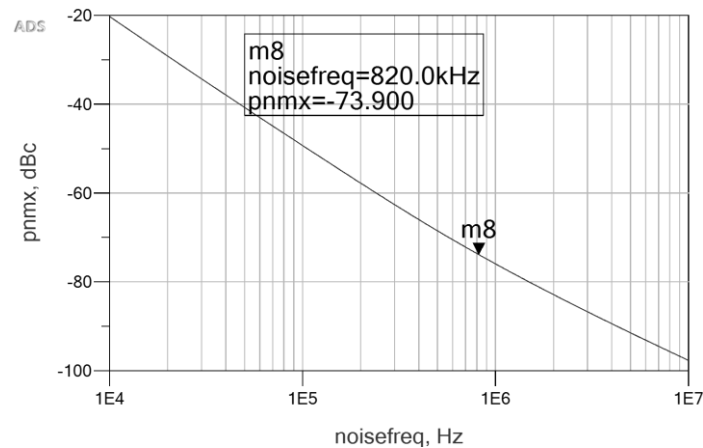
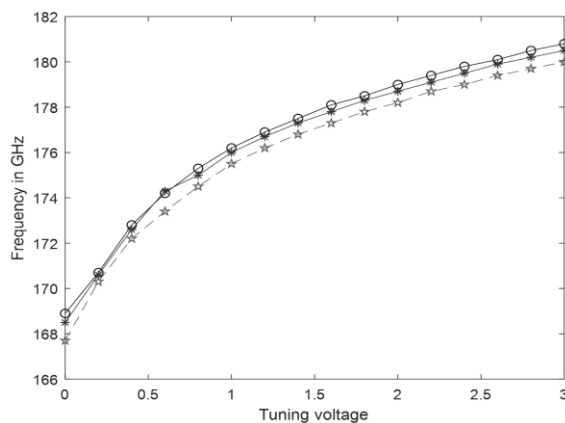
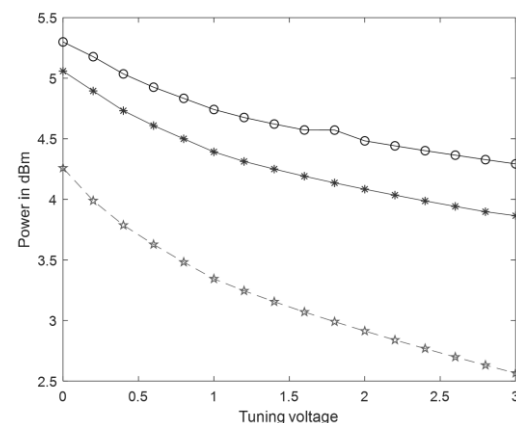


Figure 9. Simulated PN

4.3. Results of tuning range

The results presented showed the tuning range and the equivalent frequency variation according to the tuning voltage range and the corresponding output power at each range. This shows the effectiveness of using voltage to control frequencies. When biased at V_{cc} of 1.6 V, a tuning range between 0 to 3 V produces a frequency variation of 168.9 to 180 GHz allowing the VCO to be able to sweep across a range of bandwidth which is a very good property of a VCO.

At higher tuning states, the transistor-based variable resonator can achieve an enhanced quality factor, which enhances the PN in general at THz frequencies. The output impedance measured will be used for conjugate matching to the input impedance of the input stage of the solid-state power amplifier (SSPA). The power, frequency, and tuning voltage of the VCO were simulated as shown in Figures 10 and 11 for three distinct bias voltages of 1.2, 1.4, and 1.6 V for a tuning voltage range from 0 to 3 V.

Figure 10. Graph of V_{tune} vs frequencyFigure 11. Graph of V_{tune} vs power (dBm)

When biased with 0.8 V, the VCO begins to oscillate at the desired center frequency, even if, as expected, the low supply voltage causes some variations in the characteristics of the VCO because the transistor runs at diverse bias points, causing the transistor's non-linear behavior to alter. In any event, as shown in the following. The bias circuitry absorbs a little amount of electricity (up to 6 mA for the higher bias voltage). The VCO's tuning curve is provided, and it reveals that, at a central frequency of 175.3 GHz, a bandwidth of 11.9 GHz was successfully attained. With a voltage sweep of 0–1.6 V, this yields a tuning range of 6.788%. Over the VCO's total tuning range, the design aspect ensures that the power output stays constant, or at least over the minimum needed value. The circuit consumes 42.6 mA with a supply voltage of 1.6 V, resulting in total power consumption of 68.18 mW. Given the VCO's overall DC-power consumption of only 68.18 mW, the peak power output of 5.3 dBm is quite considerable. As shown in Figure 12, the flatness or amplitude fluctuation of only 1.01 dBm at 1.6 V over frequency is excellent. The capacity to

generate a high-power, adjustable signal with extremely high efficiency is a fundamental characteristic of the developed VCO. Table 4 shows a thorough comparison of the produced results with various literary solutions.

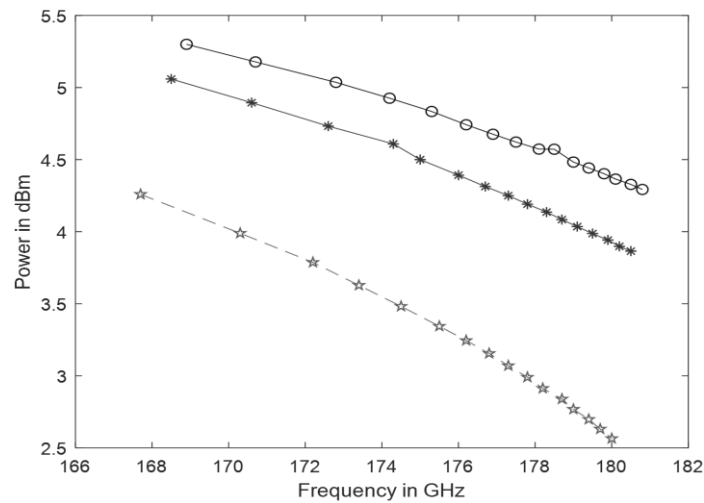


Figure 12. Simulated differential power output against frequency

Table 4. Table of comparison of results

	[23]	[24]	[25]	[26]	[27]	[28]	This work
Technology	130 nm SiGe HBT	0.25 nm SiGe	130 nm SiGe HBT	130 nm SiGe HBT	55 nm SiGe HBT	130 nm SiGe HBT	130 nm SiGe HBT
Center frequency (GHz)	184	161	190.6	140	195	176	175.3
Tuning percentage (%)	2	4.7	NA	NA	2	NA	6.788
Tuning bandwidth (GHz)	NA	NA	12.2	NA	NA	8.5	11.9
PN @ (frequency offset)	NA	-86 @1	-91 @ 10	-75 @1	98.6 @1	-110 @10	73.9 @ 10
MHz, dBc/Hz							
Power output (dBm)	-11	-20	3.2	-1.5	6.5	7.3	7.8
Chip dimension (mm ²)	NA	NA	0.70×0.33	0.275	NA	0.30×0.35	
Power consumption (mw)	NA	NA	16.2	47	25.8	82	68.18

5. CONCLUSION

Due to the vast uses in medical imaging that THz frequencies can provide, the design of a differential 175 GHz SiGe-based VCO with greater than 7.6 dBm power was accomplished in this work. The development of high-power, integrated THz sources that operate inside the THz atmospheric transmission windows is one of the main challenges to attaining any of the uses. With an extensive examination of parasitics, mathematical analysis of load impedances, and implementation of the differential design. The PN was reduced, and the output power was enhanced. Simulations were performed using ADS keysight 2019 and power out of 7.8 dBm, PN of -73 @ 10 MHz offset, a tuning range of 11.9% and power consumption of 68.18 mw results were achieved. This is an increment of 6.85% in power output, 40% in the tuning range, 17% reduction in DC power consumption, and 33% reduction in PN compared to the past works cited.




REFERENCES

- [1] Z. Li, B. Qi, X. Zhang, S. Zeinolabedinzadeh, L. Sang, and J. D. Cressler, "A 0.32-THz SiGe imaging array with polarization diversity," *IEEE Transactions on Terahertz Science and Technology*, vol. 8, no. 2, pp. 215–223, Mar. 2018, doi: 10.1109/TTHZ.2017.2787958.
- [2] A. J. Fitzgerald, E. Berry, N. N. Zinovev, G. C. Walker, M. A. Smith, and J. M. Chamberlain, "An introduction to medical imaging with coherent terahertz frequency radiation," *Physics in Medicine and Biology*, vol. 47, no. 7, pp. 67–84, Apr. 2002, doi: 10.1088/0031-9155/47/7/201.
- [3] Y. Bai, "Improving resolution by the higher-order microscope imaging system with thermal light," in *2014 XXXIth URSI General Assembly and Scientific Symposium (URSI GASS)*, Aug. 2014, pp. 1–3, doi: 10.1109/URSIGASS.2014.6929412.
- [4] K. B. Cooper *et al.*, "A high-resolution imaging radar at 580 GHz," *IEEE Microwave and Wireless Components Letters*, vol. 18, no. 1, pp. 64–66, Jan. 2008, doi: 10.1109/LMWC.2007.912049.
- [5] C. Hoyer, J. Wagner, and F. Ellinger, "A 60 GHz VCO with 654 MHz direct frequency modulation bandwidth in 0.13- μ m SiGe




- BiCMOS,” in *2021 International Conference on Electrical, Computer, Communications and Mechatronics Engineering (ICECCME)*, Oct. 2021, pp. 1–4, doi: 10.1109/ICECCME52200.2021.9591117.
- [6] R. Bindiganavile and A. Tajalli, “A controllable KVCO ring VCO topology,” in *2021 IEEE International Midwest Symposium on Circuits and Systems (MWSCAS)*, Aug. 2021, pp. 732–736, doi: 10.1109/MWSCAS47672.2021.9531824.
- [7] J. Raab *et al.*, “Ultrafast two-dimensional field spectroscopy of terahertz intersubband saturable absorbers,” *Optics Express*, vol. 27, no. 3, pp. 2248–2257, Feb. 2019, doi: 10.1364/OE.27.002248.
- [8] M. B. Wallace, A. Wax, D. N. Roberts, and R. N. Graf, “Reflectance spectroscopy,” *Gastrointestinal Endoscopy Clinics of North America*, vol. 19, no. 2, pp. 233–242, Apr. 2009, doi: 10.1016/j.giec.2009.02.008.
- [9] Z. Vafapour, A. Keshavarz, and H. Ghahraloud, “The potential of terahertz sensing for cancer diagnosis,” *Heliyon*, vol. 6, no. 12, pp. 1–8, Dec. 2020, doi: 10.1016/j.heliyon.2020.e05623.
- [10] P.-Y. Chiang, O. Momeni, and P. Heydari, “A 200-GHz inductively tuned VCO with 7-dBm output power in 130-nm SiGe BiCMOS,” *IEEE Transactions on Microwave Theory and Techniques*, vol. 61, no. 10, pp. 3666–3673, Oct. 2013, doi: 10.1109/TMTT.2013.2279779.
- [11] O. Momeni and E. Afshari, “High power terahertz and millimeter-wave oscillator design: A systematic approach,” *IEEE Journal of Solid-State Circuits*, vol. 46, no. 3, pp. 583–597, Mar. 2011, doi: 10.1109/JSSC.2011.2104553.
- [12] S. Voinigescu, *High-frequency integrated circuits*. Cambridge: Cambridge University Press, 2013.
- [13] M. Schroter *et al.*, “The EU DOTSEVEN project: Overview and results,” in *2016 IEEE Compound Semiconductor Integrated Circuit Symposium (CSICS)*, Oct. 2016, pp. 1–4, doi: 10.1109/CSICS.2016.7751070.
- [14] F. Ahmed, M. Furqan, B. Heinemann, and A. Stelzer, “0.3-THz SiGe-based high-efficiency push–push VCOs with > 1-mW peak output power employing common-mode impedance enhancement,” *IEEE Transactions on Microwave Theory and Techniques*, vol. 66, no. 3, pp. 1384–1398, Mar. 2018, doi: 10.1109/TMTT.2017.2767593.
- [15] A. Bhat and N. Krishnapura, “26.3 A 25-to-38 GHz, 195 dB FoMT LC QVCO in 65 nm LP CMOS using a 4-port dual-mode resonator for 5G radios,” in *2019 IEEE International Solid-State Circuits Conference (ISSCC)*, Feb. 2019, pp. 412–414, doi: 10.1109/ISSCC.2019.8662502.
- [16] L. Pantoli, H. Bello, G. Leuzzi, H. J. Ng, and D. Kissinger, “SiGe sub-THz VCOs design approach for imaging applications,” in *2020 International Workshop on Integrated Nonlinear Microwave and Millimetre-Wave Circuits (INMMiC)*, Jul. 2020, pp. 1–3, doi: 10.1109/INMMiC46721.2020.9160077.
- [17] C.-C. Chuang and H.-K. Chiou, “A low phase noise X band class E power VCO in 0.25 μm GaN/SiC technology,” in *2021 IEEE International Symposium on Radio-Frequency Integration Technology (RFIT)*, Aug. 2021, pp. 1–3, doi: 10.1109/RFIT52905.2021.9565205.
- [18] G. Gonzalez, *Foundations of oscillator circuit design*. Norwood: Artech House, 2007.
- [19] H. Wang, J. Chen, J. T. S. Do, H. Rashtian, and X. Liu, “High-efficiency millimeter-wave single-ended and differential fundamental oscillators in CMOS,” *IEEE Journal of Solid-State Circuits*, vol. 53, no. 8, pp. 2151–2163, Aug. 2018, doi: 10.1109/JSSC.2018.2837863.
- [20] S. Kong, H. Liu, Y. Shen, Y. Wu, Y. Yu, and K. Kang, “A 3.65–4.10 GHz class-C VCO with 189.1 DBC/hz FoM based on low electromagnetic coupling,” in *2021 International Conference on Microwave and Millimeter Wave Technology (ICMMT)*, May 2021, pp. 1–3, doi: 10.1109/ICMMT52847.2021.9618554.
- [21] Y. Z. M. Ibrahim, M. A. Y. Abdalla, and A. N. Mohieldin, “A 197 FOMT VCO with 34% tuning range for 5G applications in 45nm SOI technology,” in *2022 IEEE Radio and Wireless Symposium (RWS)*, Jan. 2022, pp. 108–110, doi: 10.1109/RWS53089.2022.9719977.
- [22] P. Maheshwari, P. K. Sadhu, M. Deharia, N. Nambath, and S. Gupta, “A quadrature-phase voltage controlled oscillator for offset phase and frequency compensation,” in *2018 31st International Conference on VLSI Design and 2018 17th International Conference on Embedded Systems (VLSID)*, Jan. 2018, pp. 177–180, doi: 10.1109/VLSID.2018.58.
- [23] F. Vogelsang, D. Starke, J. Wittemeier, H. Rucker, and N. Pohl, “A highly-efficient 120 GHz and 240 GHz signal source in a SiGe-technology,” in *2020 IEEE BiCMOS and Compound Semiconductor Integrated Circuits and Technology Symposium (BCICTS)*, Nov. 2020, pp. 1–4, doi: 10.1109/BCICTS48439.2020.9392945.
- [24] Y. Zhao, B. Heinemann, and U. R. Pfeiffer, “Fundamental mode colpitts VCOs at 115 and 165-GHz,” in *2011 IEEE Bipolar/BiCMOS Circuits and Technology Meeting*, Oct. 2011, pp. 33–36, doi: 10.1109/BCTM.2011.6082744.
- [25] D. Fritsche, S. Li, N. Joram, C. Carta, and F. Ellinger, “Design and characterization of a 190-GHz voltage-controlled oscillator,” in *2016 46th European Microwave Conference (EuMC)*, Oct. 2016, pp. 493–496, doi: 10.1109/EuMC.2016.7824387.
- [26] U. Ali, G. Fischer, and A. Thiede, “Low power fundamental VCO design in D-band using 0.13 μm SiGe BiCMOS technology,” in *2015 German Microwave Conference*, Mar. 2015, pp. 359–362, doi: 10.1109/GEMIC.2015.7107827.
- [27] B. Khamaisi and E. Socher, “A 159–169 GHz frequency source with 1.26 mW peak output power in 65 nm CMOS,” in *2013 European Microwave Conference*, 2013, pp. 536–539, doi: 10.23919/EuMC.2013.6686955.
- [28] H. Bello, L. Pantoli, H. J. Ng, D. Kissinger, and G. Leuzzi, “Low phase-noise high output power 176-GHz voltage-controlled oscillator in a 130-nm BiCMOS technology,” *IET Microwaves, Antennas & Propagation*, vol. 13, no. 14, pp. 2490–2494, Nov. 2019, doi: 10.1049/iet-map.2019.0397.

BIOGRAPHIES OF AUTHORS






Oluseun Damilola Oyeleke    is a lecturer 1 at the Nile University of Nigeria. He is a graduate of Electrical engineering from Bayero University Kano and also has his Meng from the Nigeria Defence Academy in Electronics and communications. His research interest is in the areas of microwave technology, solid-state electronics, and machine learning for telecommunication and health applications. He can be contacted at email: oluseun.oyeleke@nileuniversity.edu.ng or contactseun@gmail.com.






Aliyu Danjuma Usman    is a Professor of Telecommunications Engineering from Ahmadu Bello University, Zaria. He obtained his Ph.D. in Electrical and Electronics Engineering, from Universiti Putra, Malaysia (UPM) in 2011. Master of Electrical Engineering from Bayero University Kano (BUK) in 2006. BSc in Computer Engineering from MAAUN in 2018. He is a recipient of numerous merit and recognition awards. His work experience span from industries to academia. He worked with the Polytechnic sector and rose to the rank of Chief lecturer before joining the University. He published over 130 peer-reviewed National and International Journals/Conferences and has authored many books and book Chapters. Currently, he has over 310 citations and 10 h-index. He is a recipient of many research grants locally and internationally. He has so far graduated over 30 M.Sc, 10 Ph.D. students and many under his supervision. He served as Technical Committee Chair and member of numerous local and international conferences. Prof. Usman is a member of many national and international professional bodies which include; IEEE, COREN, MNSE, and MSESN. Research interest: teletraffic engineering, antenna radiation, wireless communications, microwave engineering terahertz frequencies, and RF EMF effect. He can be contacted at email: adusman@abu.edu.ng; aliuyusman1@gmail.






Kabir Ahmad Abubila    is a Professor at the Department of Telecommunications Engineering, Ahmadu Bello University, Zaria. He received his B. Engr, M.Sc, and Ph.D. Degrees from Department of Electrical Engineering, Ahmadu Bello University Zaria, Nigeria, in 2006, 2009, and 2015, respectively. He has several publications and Conference proceedings. He won the best student paper award at the 2013 International Conference of Electrical and Electronics Engineering at the World Congress of Engineering, London 2013. His research interests are wireless and mobile communications, microcontrollers and applications, and digital electronics. He can be contacted at email: kabirahmed@abu.edu.ng; kb.ahmad74@gmail.com.



Habeeb Bello    holds a Ph.D. in Electrical, Electronics, and Information Engineering from the University of L'Aquila, Italy in 2019, a Master's degree in Communication Engineering from The University of Manchester, United Kingdom in 2015, and he also worked as a guest research scientist in the circuit department, Innovation for High-performance microelectronics (IHP), Frankfurt (Oder), Germany and Technical University of Denmark (DTU), Denmark. Habeeb received his B.Eng in Electrical and Computer Engineering from the Federal University of Technology, Minna, Nigeria. His research interest includes communications systems, radar systems, antenna design, millimeter-wave, and THz integrated circuits for imaging and communication applications. He is currently a staff of the Department of Electronics and Telecommunications Engineering, Ahmadu Bello University, Zaria, Nigeria. He can be contacted at email: bello.habeeb@abu.edu.ng.



Olabode Idowu-Bismark    holds a B.Eng. in Electrical and Electronics Engineering from the University of Benin, in Nigeria. M.Sc degree in Telecommunications Engineering from Birmingham University UK and a Ph.D. in Information and Communication Engineering from Covenant University, Ota, Nigeria. Olabode has worked in various companies including Logic Sciences Limited, Basscomm, and Primotek Systems Limited as a senior engineer, project manager, and executive director. He is a member of the Nigerian Society of Engineers, MIEEE, and a COREN Registered Engineer. His research interest is in the area of mobile communication, mmWave, and MIMO communication. He has published many scientific papers in international peer-reviewed journals and conferences. He can be contacted at email: idowubismarkolabode@gmail.com.